

Advection-dominated Accretion in the Galactic Center and the Appearance of Sgr A*

Thomas Beckert and Wolfgang J. Duschl¹

*Institut für Theoretische Astrophysik, Universität Heidelberg,
Tiergartenstr. 15, 69121 Heidelberg, Germany*

Abstract. We present a modified description of advection-dominated accretion flows with a geometrical viscosity. A simplified treatment of the dynamics of the flow in the inner relativistic part is suggested and results are compared with the galactic center source Sgr A*.

1. Introduction

The existence of a massive black hole in the Galactic Center is a keystone in the understanding of stellar dynamics in the inner parsec of the galaxy (see the contributions of Ghez and Eckart in this volume) as it is a test case for the theory of accretion flows in active and non-active galactic nuclei (Mezger, Duschl & Zylka, 1996). Standard thin accretion disks fail to explain the luminosity and spectrum of the radio source Sgr A* and several models for the accretion and emission processes have been suggested. Optically thick synchrotron emission from a jet-disk system (Falcke et al., 1996) or from an advection-dominated accretion flow (ADAF) were investigated (Narayan et al., 1998), while optically thin emission by highly relativistic particles with a quasi-monoenergetic distribution (e.g. Beckert & Duschl 1997) is also a possible mechanism. Mahadevan (1998, and this volume) propose secondary electrons from pion decay in ADAF's as the synchrotron emitting particles and showed a way to connect the accretion flow as an energy source with the relativistic electrons. We present a simplified relativistic treatment of advection-dominated accretion in the galactic center and propose a switch between standard and ADAF accretion to distinguish AGN's and sub-luminous galactic centers.

2. Dynamics of Advection-dominated Accretion into Black Holes

Advection dominated accretion flows are geometrically thick and a description in spherical coordinates is appropriate. In order to avoid complications due to frame dragging by a rotating black hole we use the Schwarzschild metric and hope to see also the characteristics of accretion into a slowly rotating hole. The effects of strong gravity and the existence of a horizon are correctly described in this way.

¹also at: MPI für Radioastronomie, Auf dem Hügel 69, 53121 Bonn, Germany

2.1. Energy Advection and Projectors

The dynamics of an accretion flow into a black hole is governed by energy and momentum conservation. Energy losses due to radiation have to be calculated and applied separately. Angular momentum is transported into the black hole and to larger radii than those under consideration so a momentum flux through the boundaries of the disk occurs. We will neglect magnetic torques in our treatment and consider only a contribution of the magnetic pressure in the flow to the total pressure by scaling it as $\beta = p_{\text{Gas}}/p_{\text{Mag}}$. The dynamics can then be derived from the divergence of the stress-energy tensor

$$T^{ij}_{;j} = 0 \quad \text{with} \quad T^{ij} = \tilde{\rho} \frac{V^i V^j}{c^2} + p g^{ij} - 2\mu D^{ij} + c^{-2} (Q^i V^j + V^i Q^j) \quad . \quad (1)$$

The density $\tilde{\rho}$ contains a contribution from the specific enthalpy of the gas like $\tilde{\rho} = \rho \left(1 + \frac{h}{c^2}\right)$ with the rest mass density ρ . V^i are the components of the 4-velocity of the flow, p the isotropic pressure and g^{ij} the metric tensor. The viscous part of the stress-energy tensor contains the kinematical viscosity $\mu = \nu\rho$ and the shear-stresses D^{ij} . We have added a contribution by a possible heat flux Q^i which has to be orthogonal to the velocity. The 0-component of the divergence in (1) is an energy equation for the flow, but does not resemble the second law of thermodynamics. This is formulated for a system at rest so we have to project the divergence in (1) onto the 4-velocity of the flow. The tool for this is a symmetric projector

$$P^{ij} = g^{ij} + c^{-2} V^i V^j \quad P^i_j (T^{jk}_{;k}) = 0 \quad . \quad (2)$$

After the projection we get an energy equation like

$$\rho T \frac{Ds}{D\tau} = 2\mu D_{ij} D^{ij} - Q^i_{;i} - c^{-2} Q_i A^i \quad . \quad (3)$$

Here we have used the substantial derivative $\frac{Ds}{D\tau} = V^j s_{,j}$ and the acceleration $A^i = \frac{DV^i}{D\tau}$. In the following we treat stationary and axisymmetric flows with radial infall.

2.2. Isothermal Poloidal Stratification

In optically thin plasma the heat produced locally by viscous friction will be either maintained as internal energy or radiated away. Diffusive transport by radiation will not occur. Instead of a radiative transport we expect turbulence driven by the magneto-rotational instability (e.g. Balbus & Hawley, 1998) to transport heat effectively perpendicular to the flow. So we approximate the poloidal structure by an isothermal plasma in hydrostatic equilibrium. The poloidal stratification is given by

$$\frac{\partial p}{\partial \theta} = \rho(1 + h/c^2) \sin \theta \cos \theta r^2 \Omega^2 \quad . \quad (4)$$

With the assumed isothermal equation of state we can integrate and obtain

$$\rho(\theta) = \rho_0 \exp \left[-\frac{\cos^2 \theta}{2} \left(\frac{r\Omega}{c_s} \right)^2 \left(1 + \frac{\epsilon}{c^2} + \left(\frac{c_s}{c} \right)^2 \right) \right] \quad . \quad (5)$$

One obtains the criterion for the flow to be a thin disk as

$$\frac{c_s^2}{1 + \frac{h}{c^2}} \ll (r\Omega)^2 \quad . \quad (6)$$

We take $c_s^2 = \frac{\partial p}{\partial \rho} \propto T$ at constant temperature for an ideal gas. The internal energy and so the enthalpy rises strongly with temperature when the particles become relativistic and the disk thickness will shrink in the relativistic inner part close to the black hole.

2.3. Momentum transport and Viscosity

In a stationary state as we are interested in the angular momentum distribution is determined by diffusive transport due to an effective turbulent viscosity

$$-\frac{\dot{M}}{2\pi} \left(\left(1 + \frac{h}{c^2}\right) \frac{\partial}{\partial r} (r^2\Omega) + \frac{r^2\Omega}{\Sigma c^2} \frac{\partial P}{\partial r} \right) = \frac{\partial}{\partial r} \left(\nu \Sigma r^3 \frac{\partial}{\partial r} \Omega \right) \quad . \quad (7)$$

For the viscosity we take a parametrisation

$$\nu = \alpha(r - r_s)v_\phi \quad \alpha \approx \mathcal{R}_c^{-1} \approx 10^{-1\dots-3} \quad (8)$$

proposed by Duschl, Strittmatter & Biermann which is discussed by R. Auer (this volume ??). For the self-similar solution of Narayan & Yi (1994) this viscosity has the same radial dependence as the standard form by Shakura & Sunyaev (1973) . Whenever the ADAF's deviate from the power-law behavior the viscosity is not coupled to the thermal state of the flow but rather to the dynamical structure¹. The parameter α is proportional to the inverse of the critical Reynolds number \mathcal{R}_c in the flow. MHD-instabilities may produce turbulence at rather small \mathcal{R} , so we take $\alpha = 0.1$. The radial momentum balance

$$\begin{aligned} & \left(\frac{Mc^2}{r^2} - \left(1 - \frac{3M}{r}\right) r\Omega^2 + v_r \frac{\partial v_r}{\partial r} \right) \left(1 + \frac{h}{c^2}\right) + \frac{\left(1 - \frac{2M}{r}\right) + \frac{v_r^2}{c^2}}{\Sigma} \frac{\partial P}{\partial r} \\ & = \frac{4}{3\Sigma} \left[\left(\frac{\partial}{\partial r} \frac{\nu \Sigma}{r} \left(\frac{\partial}{\partial r} r v_r \right) \right) - \frac{2v_r}{r} \left(\frac{\partial}{\partial r} \nu \Sigma \right) \right] \end{aligned} \quad (9)$$

includes the viscous braking in a converging flow and the inertia and pressure terms. The centrifugal force reverses sign at $r = 3M = 3/2R_S$. The length scale $M = GM/c^2$ is the gravitational radius with \mathcal{M} the mass of the black hole.

2.4. Heating and Cooling of the Flow

The thermal balance in a stationary state is given by

$$Q_{\text{adv}} = Q_{\text{vis}}^+ - Q_{\text{heat}} - Q^- \quad . \quad (10)$$

¹The length scale over which angular momentum is transported by eddie-exchange is limited by the distance to the horizon at r_s .

The flow cools via bremsstrahlung, synchrotron- and inverse Compton losses (Q^-), while the disk is heated by viscous friction

$$Q_{\text{vis}}^+ = \nu \Sigma r^2 \left[\frac{4}{3} \left(\frac{\partial}{\partial r} \left(\frac{v_r}{r} \right) \right)^2 + (\partial_r \Omega)^2 \right] \quad (11)$$

and the divergence of a possible heat flux Q_{heat} . The heat flux in collisionless plasma is approximated by $Q_{\text{heat}} = \Phi \Sigma c_s^3$. In a magnetized plasma the heat flux is expected to be strongly depressed so we take $\Phi = 10^{-3}$. The heat generated in the flow is not completely radiated but is advected with the flow according to

$$Q_{\text{adv}} = \Sigma v_r c_V \left[\frac{\partial T}{\partial r} - (\Gamma_3 - 1) \frac{T}{\rho} \frac{\partial \rho}{\partial r} \right] \quad (12)$$

The thermodynamic quantities c_V, Γ_3 are taken from the relativistic equation of state for an ideal gas. The thermal balance must be treated for electrons and ions separately with an exchange of heat between the two species. This is assumed to occur only by Coulomb collisions but is subject to debate, as energy transfer due to resonant scattering of electrons by whistler waves can not be excluded.

3. Numerical Treatment

The vertically averaged dynamical equations for stationary flows presented above allow for a self-similar solution in the Newtonian limit and a constant advection ratio (Narayan & Yi, 1994), so that $Q_{\text{adv}} \propto Q_{\text{vis}}^+$ replaces the energy equation (10). The self-similarity implies constant logarithmic gradients for all variables

$$\frac{d\Omega}{dr} = \left(\frac{d \ln \Omega}{d \ln r} \right) \frac{\Omega}{r} \quad (13)$$

as shown here for the angular velocity. The differential equations are decoupled and one obtains a set of algebraic equations, which can be easily solved. We use a logarithmic radial grid and solve the algebraic equations with the full energy balance at all points. From the local solutions we recalculate the actual logarithmic gradients for a next iteration step. In doing so we avoid inner regularity conditions at critical (sonic) points. The steep gradients present in the solutions at 3 Schwarzschild radii (Fig. 1) lead to a slow convergence and the solutions shown are not completely relaxed to a stationary state. The cooling of the flow by radiation is unimportant at very small accretion rates and the radiation processes have no backreaction on the dynamics of the flow. We include bremsstrahlung, synchrotron and inverse Compton-scattered synchrotron radiation in a rough approximation in the energy equation and derive the spectra from the ADAF-solutions afterwards.

4. Mass Accretion in the Galactic Center

The accretion rate necessary to power the galactic center source Sgr A* is $10^{-9} \dots 10^{-10} M_{\odot}/\text{yr}$ for a thin accretion disk. But upper limits from IR-measurements allow only a mass flux of $10^{-11} M_{\odot}/\text{yr}$ or lower. The inefficiency of

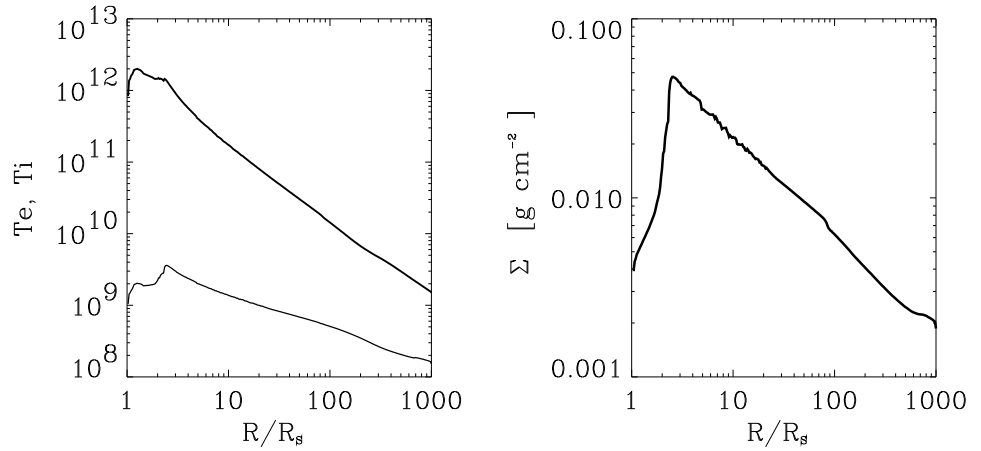


Figure 1. Electron (lower curve) and ion temperatures (upper curve) as a function of radius and the surface density of an ADAF with a mass flow rate of $10^{-5} M_{\odot}/\text{yr}$. Density and temperatures deviate significantly from the self-similar form at the last stable circular orbit at $3R_S$ where angular momentum does not provide a potential barrier anymore.

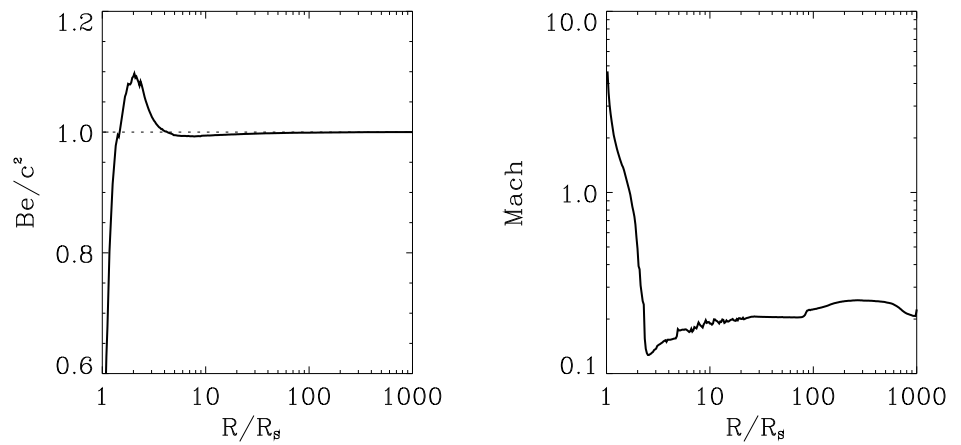


Figure 2. Specific Bernoulli number and radial Mach number of the flow. The Bernoulli number includes the rest mass of the particles, so a zero-energy flow has a Bernoulli number of 1. The Mach number shows a transition from subsonic to supersonic behavior inside the last stable circular particle orbit.

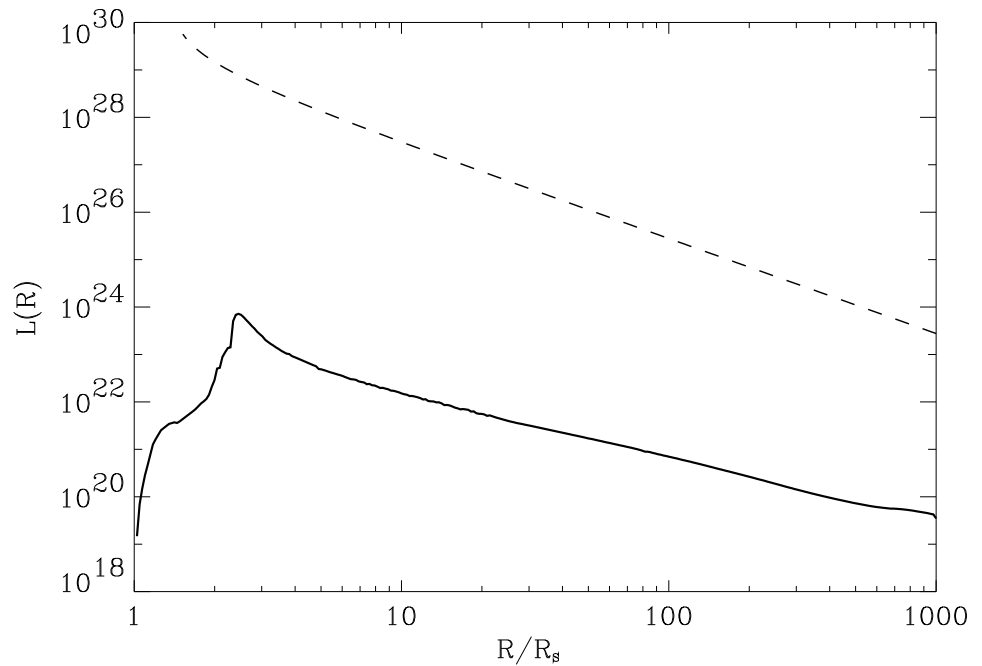


Figure 3. Local luminosity of ADAF and standard thin accretion disk for a mass accretion rate of $10^{-5} M_{\odot}/\text{yr}$. The thin disk luminosity (dashed line) is considerably larger than the ADAF emission (solid line) and ends at 1.5 black hole radii, where the centrifugal force reverses its direction and is unable to support a stationary thin flow.

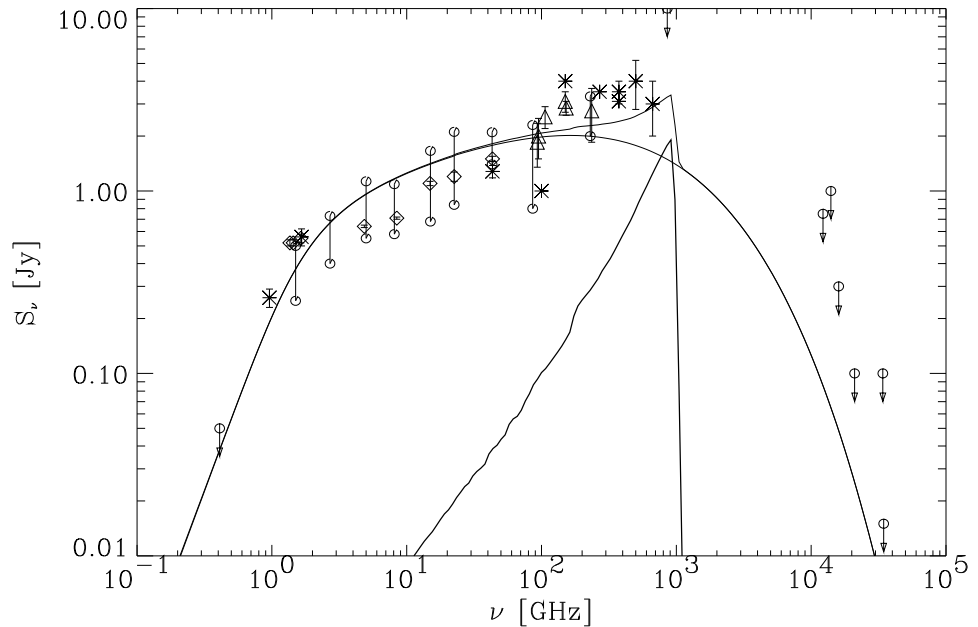


Figure 4. A comparison between minimal ADAF model and radio-IR observations. We have combined single measurements with variability ranges marked by symbols with circles at both ends. The emission by the ADAF itself peaks at 10^3 GHz. Optically thin synchrotron emission from relativistic electrons provide the flux at almost all other frequencies. The combined spectrum is also shown and falls a little short for the measured flux at 100-1000 GHz.

ADAF-emission processes point to much larger accretion rates, which are determined from a simultaneous fit of sub-mm and X-ray measurements. The critical parameters are the mass of the black hole, here $\mathcal{M} = 2.6 \cdot 10^6 M_{\odot}$, the distance to the galactic center $D = 8$ kpc and the hydrogen column density for soft X-ray absorption $N_{\text{H}} = 6 \cdot 10^{21} \text{ cm}^{-2}$. We assume that most radio observations are dominated by optically thin synchrotron emission from relativistic electrons and the ADAF contributes significantly in the sub-mm regime only. This minimal ADAF-model is calculated with a plasma- $\beta = 10$ and is correspondingly gas pressure dominated. The derived mass accretion rate is $1 \cdot 10^{-5} M_{\odot}/\text{yr}$. Temperatures and surface density of this model is shown in Fig. 1. In contradiction to the analytical solutions and Narayan & Yi (1995) we find Bernoulli numbers less than 1, corresponding to the rest mass at infinity as seen in Fig. 2. The radiation inefficiency is shown in Fig. 3, where the local luminosity is compared to the luminosity of a thin disk at the same accretion rate.

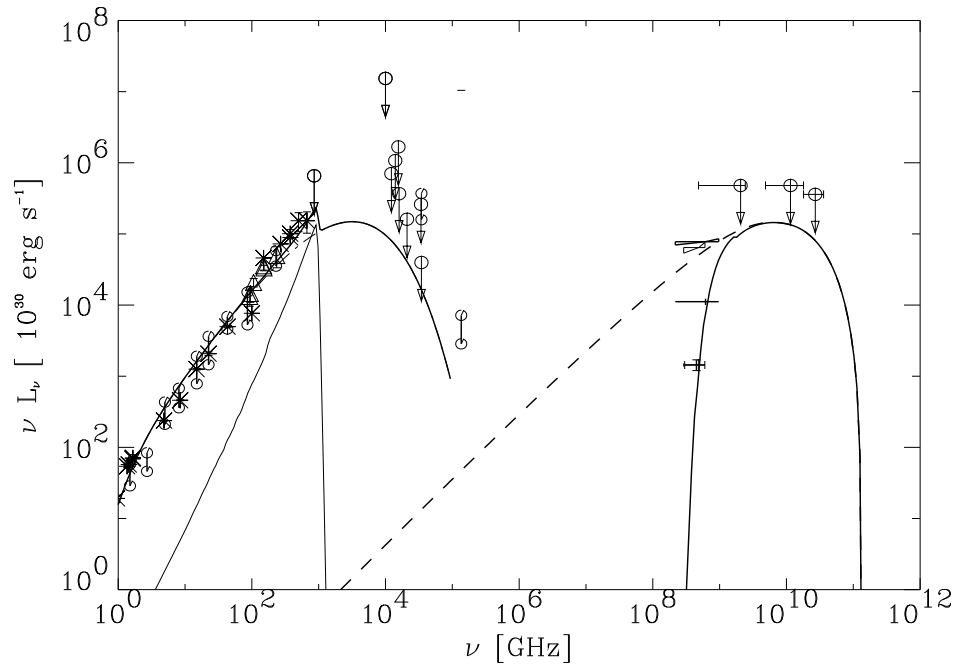


Figure 5. The radio to X-ray emission of Sgr A* and the minimal ADAF-model. ROSAT, *Einstein* and GINGA observations are included. Both the uncorrected and the corrected fluxes corresponding to a column density of $N_{\text{H}} = 6 \cdot 10^{21} \text{ cm}^{-2}$ are shown. The intrinsic spectrum of free-free emission is given by the dashed line. According to our model most radio observations see optically thin synchrotron emission, but the energy output is dominated by the ADAF, both in the sub-mm and X-ray regime. The comptonized synchrotron emission emerges at IR-optical frequencies and is not included.

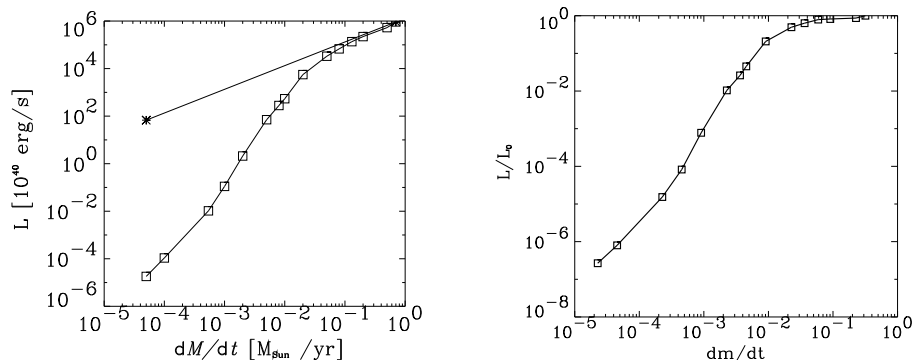


Figure 6. The total luminosity of standard (upper line) and ADAF's as a function of mass accretion rate (left plot) for a $10^8 M_{\odot}$ black hole. Squares mark calculated luminosities of ADAF's in our treatment. The relative luminosity of ADAF's versus \dot{M} in units of the Eddington accretion rate shows the rapid deviation of ADAF's from the standard disk luminosity within two decades in the mass flow rate.

5. Synchrotron and X-ray Spectrum of Sgr A*

The optically thick self-absorbed synchrotron radiation of the ADAF emerges in the radio and sub-mm regime and rises steeply to a maximum at 10^3 GHz. It shows an even steeper cut-off for larger frequencies seen in Fig. 5. Most of the radio observations can not be explained by the ADAF itself. One possible source for this radiation are relativistic electrons of $E = 203$ MeV emitting optically thin synchrotron radiation in a weak magnetic field $B = 2.8$ G. Assuming a homogeneous source its radius is at least $R = 4.5 \cdot 10^{13}$ cm, much larger than the synchrotron emitting region of the ADAF and thus providing an extended halo. These relativistic electrons can be accelerated in magnetic reconnection sheets (Schopper, Lesch & Birk, 1998) and maintained in a quasi-monoenergetic distribution (Jauch, this volume) or they may be secondary electrons from charged pion decays (Mahadevan, 1998).

6. How to switch on an AGN and how to switch it off again

For mass accretion rates below $0.1 M_{\text{Edd}}$ there are two possible states of accretion into black holes. The standard thin disk (Frank, King & Raine, 1992), which loses all the energy produced by viscous friction locally, and the advection-dominated accretion flow (ADAF) described above. When we compare the radially integrated luminosity of the two kinds of accretion flows at the same accretion rate, we find roughly the same luminosity for a critical mass flow rate of $\alpha^2 \dot{M}_{\text{Edd}}$. At smaller rates the luminosity of ADAF's drop dramatically, while the luminosity of efficiently radiating flows is proportional to the mass accretion rate $L_0 = \eta \dot{M} c^2$. The ratio of the luminosities for ADAF's to L_0 gives the

amount of specific energy advected into the black hole and the inefficiency of the heat transfer between electrons and ions.

As both states of accretion are available at the same time in a stationary flow, there must be a physical reason, which enforces the flow to be advection-dominated or not. If a mechanism is at work deciding in which state the flow will be, it provides a switch to turn a luminous accreting black hole into a quiet sink of matter or the other way round.

Let us, for the moment being, assume that, whenever available, an accretion disk chooses to operate in the advection dominated regime, which is indicated by the extremely low luminosity of the Galactic Center. Then comparatively small changes in the mass flow rate through the disk may result in dramatic changes of the efficiency of the accretion process, i.e., the luminosity of the AGN. This highly non-linear behaviour of the luminosity as a function of the accretion rate has the potential of acting almost as a switch between an AGN phase of a galaxy and a non-active phase without having to change the mass flow rate by a similar amount as the luminosity. In our example of Fig. 6, at a mass flow rate of $\sim 10^{-4} M_{\odot}/\text{yr}$ an increase of the rate by two orders of magnitude results in almost a million times larger a luminosity.

Acknowledgments. This work was supported by the DFG through SFB 328 *Evolution of Galaxies*.

References

- Balbus S. A., Hawley J. F., 1998, *Reviews of Modern Physics* 70, 1
Beckert T., Duschl W. J., 1997, *A&A*328, 95
Falcke H., Biermann P. L., 1996, *A&A*308, 321
Frank J., King A., Raine D., *Accretion Power in Astrophysics*, 2. ed., Cambridge: University Press, 1992
Mahadevan R., 1998, *Nature* 394, 651
Mezger P. G., Duschl W. J., Zylka R., 1996, *A&AR* 7, 289
Narayan R. & Yi I., 1994, *ApJ*428, L13
Narayan R. & Yi I., 1995, *ApJ*452, 711
Narayan R., Mahadevan R., Grindlay J. E., Popham R. G., Gammie C., 1998, *ApJ*492, 554
Schopper R., Lesch H., Birk G. T., 1998, *A&A*335, 26